Tartu University

Faculty of Science and Technology

Master thesis

Model of a Self-Oscillating Ionic Polymer-Metal Composite Bending Actuator

Deivid Pugal

Supervisors: Prof. Kwang J. Kim
Res. fel. Heiki Kasemägi

Tartu 2008

Contents

Chapter 1

Publications

CC and SPIE publications related to the thesis:

- Pugal, D.; Kim, K.J.; Punning, A.; Kasemägi, H.; Kruusmaa, M.; Aabloo, A. (2008). A self-oscillating ionic polymer-metal composite bending actuator. Journal of Applied Physics, 103(8), 084908
- Kim, D.; Kim, K. J.; Tak, Y.; Pugal, D.; Park, Il-S. (2007). Self-oscillating electroactive polymer actuator. Applied Physics Letters, 90, 184104
- Pugal, D.; Kasemägi, H.; Kim, Kwang J.; Kruusmaa, M.; Aabloo, A. (2007). Finite element simulations of the bending of the IPMC sheet. Electroactive Polymer Actuators and Devices (EAPAD) (65240B).Spie - International Society For Optical Engineering

Publications not covered in the thesis:

- Pugal, D.; Kasemägi, H.; Kruusmaa, M., Aabloo, A. (2008). An advanced finite element model of IPMC. In: Electroactive Polymer Actuators and Devices (EAPAD): (Toim.) Bar-Cohen, Y.. Spie - International Society For Optical Engineering, 2008, (6927), 692711.
- Listak, Madis; Pugal, Deivid; Kruusmaa, Maarja (2007). Biomimetic fish-like underwater robot for shallow water applications. 13th International Conference on Advanced Robotics , Korea, Jeju, 21-24 August, 2007. IEEE, 2007, 332 - 336.
- Listak, Madis; Pugal, Deivid; Kruusmaa, Maarja (2007). Computational Fluid Dynamics Simulations of a Biomimetic Underwater Robot. 13th International Conference on Advanced Robotics , Korea, Jeju, 21-24 August, 2007. IEEE, 2007, 314 - 319.
- Listak, M.; Martin, G.; Pugal, D.; Aabloo, A.; Kruusmaa, M. (2005). Design of a semiautonomous biomimetic underwater vehicle for environmental monitoring. 6th IEEE International Symposium on Computational Intelligence in Robotics and Automation (CIRA 2005); Espoo, Finland; 27.06.-30.06.2005. New York: IEEE, 2005, 9 - 14.

Chapter 2

Introduction

In this thesis I consider simulations of ionic polymer-metal composite [1] (IPMC) type materials. IPMC is one kind of electroactive polymer (EAP) among others such as ferroelectric polymers [2], conducting polymers [3], carbon-nanotubes [4], dielectric elastomers [5], and ionic polymeric gels [6]. Given materials are valuable for many applications from micro robotics to military and space applications. Among many advantages of EAP materials are light weight, noiseless actuation, simple mechanics and large displacement. In addition some EAPs, such as IPMCs, are able to function in aqueous environments. Those qualities make the materials possible to use as artificial muscles.

IPMC materials are highly porous polymer materials such as Nafion^{TM}, filled with a ionic conductive liquid. There are water based IPMCs which operate in aquatic environment and current is caused by ions such as $Na+$, $K+$ dissociated in water. Other kind of IPMCs - ionic liquid based, do not need wet environment for operating. A sheet of an ionic polymer is coated with a thin metal layer, usually platinum or gold. All freely mobile cations inside the polymer migrate towards an electrode due to an applied electric field, causing expansion of the material at the one end of the sheet and contraction at the other end, which results in bending of the sheet.

In this thesis I give an short overview of different types of models used to simulate bending of an IPMC. Then I propose a general model for an IPMC. The model is extended to simulate electrochemical oscillations on the surface of an IPMC. The simulated data is validated against experimental data. The next section gives a brief overview of IPMC oscillations and my model.

2.1 Overview of the Model

The primary goal of current work is to develop an extendable Finite Element model for simulating an IPMC muscle. The model consists of two parts - one is a base model which could be used for simulating simple deflection of an IPMC. The base model is based on physics, i.e. the underlying equations describe physical processes instead of being mere extrapolation of experimental data.

There are only few Finite Element models developed for IPMC materials whereas it is possible to find rather many electromechanical models. One of the reasons could be that it is more difficult to relate experimental data to a model in case of Finite Element simulations. However, Finite Element Modelling (FEM) is very good for simulating coupled problems such as mass transfer, mechanics, electrochemistry, and etc, but it is generally not suitable for molecular scale simulations. Therefore the model which is described in next chapters uses macro scale equations of different domains such as Nernst-Planck equation for mass transfer and continuum mechancis equations to describe bending.

The second part of the model is an extension to the base model. It describes the electrochemical reactions and oscillating movement of an IPMC muscle. A series of tests with IPMCs immersed in formaldehyde (HCHO) solution has been conducted by Kim et al. [7]. Measurements under constant electric field showed current oscillations and thus also material oscillations from onset potential of $0.75V$. Therefore the second part of my model consists of four time-dependent differential equations, which describe the electrochemical reactions on the surface of an IPMC. The goal is to extend the base model to simulate a real experiment - a self-oscillating IPMC. Therefore the final model consists of the base model and electrochemistry model coupled together. The model is also validated against experimental data. The results of this thesis have also been published in Applied Physics Letters [7] and Journal of Applied Physics [8].

Chapter 3

Overview

There are several models available to describe tip displacement of an IPMC. For instance Newbury and Leo [9]proposed a linear model with mechanical terms - mechanical impedance and inertia, and two electric terms - DC resistance and charge storage. The model was based on an equivalent circuit representation that was related to the mechanical, electrical and electromechanical properties of the material. Expressions for the quasi-static and dynamic mechanical impedance were derived from beam theory. The electrical impedance was modeled as a series combination of resistive and capacitive elements. So the resulting linear electromechanical model was based on the measurement of the effective permittivity, elastic modulus, and effective strain coefficient.

There are more lumped models available. In those models input parameters such as voltage or current are converted to the output parameters - tip displacement, force, and etc. For instance Jung et al. modeled an IPMC as a high pass filter, using series of resistors and capacitors in their calculations [10]. The model was an equivalent electrical circuit model for the IPMC actuator using experimental data.

Punning proposed a non-linear transmission line model, where all the elements of transmission line had a physical meaning [11]. He showed that the IPMC model works as a delay line with changing resistors and the curvature of the IPMC sample at a given point depends on the surface resistance.

There are few Finite Element models for an IPMC available. Some authors like Wallmersperger [12] and Nasser [13] have already simulated mass transfer and electrostatic effects - similar approach is used in current thesis. Toi [14] proposed a Finite Element model, where viscosity terms in transportation processes were included explicitly. However, the basis of the described model was a rectangular beam with 2 pairs of electrodes. My approach for simulating mechanical bending is taking advantage of the numerical nature of FEM problems - the continuum mechanics equations are used instead of analytical Euler beam theory which is more commonly used by authors like Lee [15] and Wallmersperger [16].

Spontaneous oscillations are a widespread phenomenon in nature. They have been studied

for large number of experiments, including electrochemical systems, such as the oxidation of metals and organic materials [17]. Electrochemical systems exhibiting instabilities often behave like activator-inhibitor systems. In these systems the electrode potential is an essential variable and takes on the role either of the activator or of the inhibitor. If certain conditions are met, an activator-inhibitor system can generate oscillations [18]. As brought out in previous chapter, a series of tests with self-oscillating IPMCs were conducted by Kim et al. [7]. The initial oscillation model for an IPMC was proposed by D. Kim [19]. It was a numerical model, which was able to predict voltage and also tip displacement for certain experimental configuration. However the model was very rigid and did not work for different HCHO concentrations. The model was based on the work of Strasser [20], which is also the base of the electrochemical model proposed in this paper.

Chapter 4

The Base Model

An IPMC sheet consists of a polymer host and a metal coating. In our experiments, we have used Nafion^{TM} 117, coated with a thin layer of platinum. Mass transfer and electrostatic simulations are done in three mechanical domains - pure backbone polymer, pure platinum coating, and mixture of polymer and platinum - some platinum diffuses into the polymer during coating process [21]. Physical properties and dimensions of pure, 2 μm thick platinum coating are considered only when calculating bending. That gives us five mechanical domains as shown in Fig. 4.1. Most simulations are carried out for an IPMC strip, $2-4$ cm long, 200 μm thick polymer, including 10 μm thick Pt diffusion region on each side, coated with 2 μm thick platinum, in a cantilever configuration - one end of the strip is fixed.

The Nernst-Planck equation describes diffusion, convection and in presence of electric field and charges, migration of the particles. The general form of the equation is

$$\frac{\partial C}{\partial t} + \nabla \cdot (-D\nabla C - z\mu F C \nabla \phi) = -\vec{u} \cdot \nabla C, \tag{4.1}$$

where C is concentration, D diffusion constant, F Faraday constant, $\vec{u}$ velocity, z charge number, ϕ electric potential, and μ mobility of species, which is found by using known relation $\mu = D/(RT)$. There T is absolute temperature and R universal gas constant. Mobile counter ions are described by Eq. (4.1). As anions are fixed, they maintain constant charge density throughout the polymer. After a voltage is applied to the electrodes of an IPMC, all free cations will start migrating towards cathode, causing current in the outer electric circuit. Because of the fact that ions cannot move beyond the boundary of the polymer, charges start to accumulate, resulting in increase of the electric field, which cancels out the applied one. The process could be described by Gauss' Law:

$$\nabla \cdot \vec{E} = -\Delta\phi = \frac{F \cdot \rho_c}{\varepsilon}, \tag{4.2}$$

where ρ_c is charge density, ε is absolute dielectric constant and E is the strength of the electric

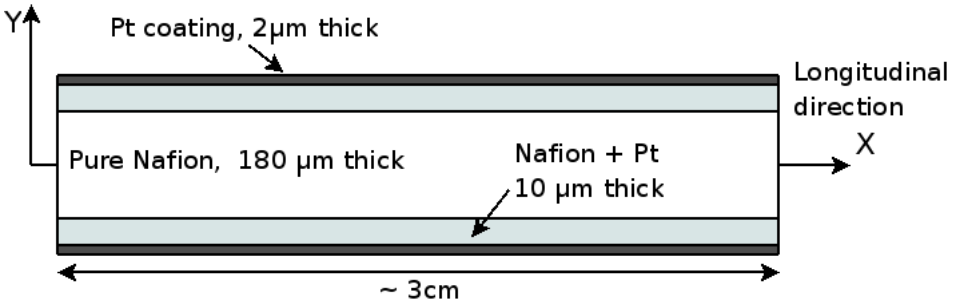

Figure 4.1: Illustration of domains and dimensions used in simulations. The length of 3 cm was used also in number of experiments. Notice that there are three different mechanical domains - pure Nafion^{TM} polymer, pure Pt coating and diffusion layer, where Pt has diffused into the polymer.

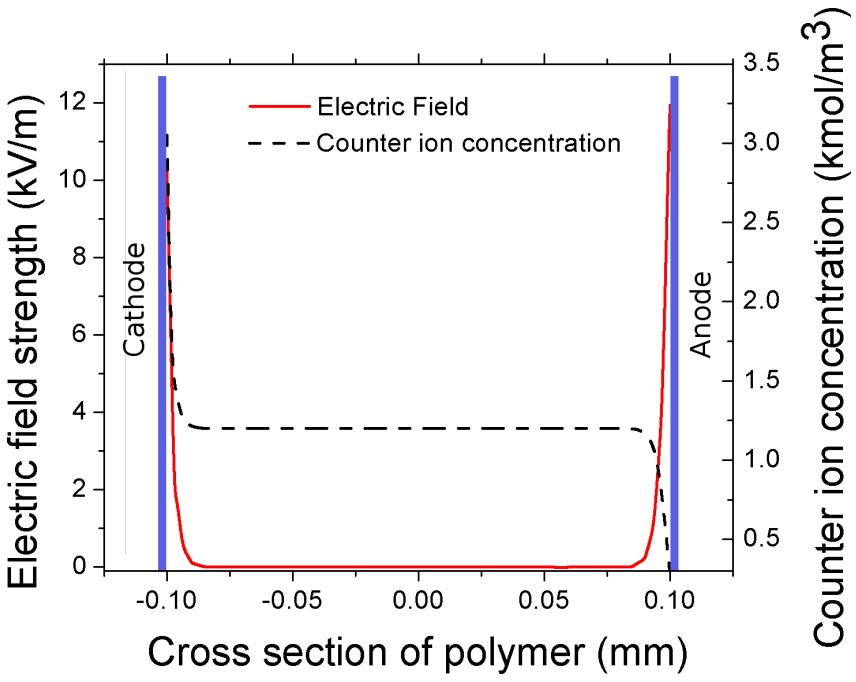

Figure 4.2: The concentration of counter ions and electric field strength inside the polymer according to simulations.

Table 4.1: Material parameters used in continuum mechanics equations.

Parameter	Value	Unit	Domain where applied
E_N	200	MPa	Nafion^{TM}
ν_N	0.49	-	Nafion^{TM}
E_{Pt}	168	GPa	Pt
ν_{Pt}	0.38	-	Pt
E_{diff}	84	GPa	Pt diffusion layer (estimated)
ν_{diff}	0.42	-	Pt diffusion layer (estimated)

field. The charge density variable is related to charge concentration:

$$\rho_c = zC + z_{anion}C_{anion}. \tag{4.3}$$

The second term in Eq. (4.3) is constant at every point of the polymer. The coupling between equations (4.1) and (4.2) is strong, i.e. no weak constraints have been used. Absolute dielectric constant ε could be explicitly written as $\varepsilon = \varepsilon_0\varepsilon_r$, where ε_0 is dielectric constant in vacuum and equals $8.85 \times 10^{-12}\ F/m$. The measured value of absolute dielectric constant ε is shown in Table 4.3. A steady state of the cations forms when electric field created by distribution of cations cancels out the applied electric field, i.e. the strength of the electric field inside the polymer is approximately zero, as also shown in Fig. 4.2. The steady state cation concentration, with average value of 1200 mol/m^3 is also shown in the same figure. It is interesting to notice that there are fluctuations in charge distribution only in really thin boundary layers, leading to the conclusion that there is no charge imbalance inside the polymer. General understanding is that locally generated charge imbalance nearby platinum electrodes is directly connected, and mainly responsible, to the bending of an IPMC [22]. Therefore we define longitudinal force per unit area at each point in the polymer of an IPMC as follows [16]:

$$\vec{F} = (A\ \rho_c + \ B\ \rho_c^2)\ \hat{x}, \tag{4.4}$$

where ρ_c is charge density and A and B are constants which are found by fitting simulations according to experimental results using system identification. Values of the constants are brought out in Table 4.3 and it is interesting to notice that the ratio A/B is close to the value suggested by Wallmersperger [16]. Equations (4.1)-(4.4) are described only for pure Nafion^{TM} and Pt diffusion domain (see Fig. 4.1). There is no ion diffusion nor migration in thin Pt coating domain.

To relate the force in Eq. 4.4 to the physical bending of an IPMC sheet, we introduce a set of continuum mechanics equations, which are effective in all domains (Fig. 4.1). These equations are described in the Comsol Multiphysics structural mechanics software package. Normal and shear strain are defined as

$$\varepsilon_i = \frac{\partial u_i}{\partial x_i},\ \varepsilon_{ij} = \frac{1}{2}\left(\frac{\partial u_i}{\partial x_j} + \frac{\partial u_j}{\partial x_i}\right), \tag{4.5}$$

Table 4.3: Parameter values used in bending simulations.

Parameter	Value	Unit
D	1×10^{-6}	cm^2/s
R	8.31	$J/(K\ mol)$
T	293	K
z	1	$-$
F	96.5×10^6	mC/mol
ε	25	mF/m
A	110	$N\ m/mol$
B	10	$N\ m^4/mol^2$
$\alpha_{polymer}$	0	s^{-1}
$\beta_{polymer}$	1.5	s

where u is the displacement vector, x denotes a coordinate and indices i and j are from 1 to 3 and denote components correspondingly to x, y, or z direction. The stress-strain relationship is

$$\sigma = D\varepsilon, \tag{4.6}$$

where D is 6×6 elasticity matrix, consisting of components of Young's modulus and Poisson's ratio. The system is in equilibrium, if the relation

$$-\nabla \cdot \sigma = \vec{F}, \tag{4.7}$$

is satisfied. This is Navier's equation for displacement. The values of Young's modulus and Poisson's ratios, which are used in the simulations, are shown in Table 4.1. The values for platinum diffusion region are not measured, but estimated as an average of values of the pure Nafion^{TM} and Pt regions.

As our simulations are dynamic rather than static, we have to introduce an equation to describe the motion of an IPMC sheet. To do that, we use Newton's Second law

$$\rho \frac{\partial^2 \vec{u}}{\partial t^2} - \nabla \cdot c\nabla \vec{u} = \vec{F}, \tag{4.8}$$

where the second term is the static Navier's equation and c is Navier constant for static Navier's equation. The first term in Eq. (4.8) introduces the dynamic part. Several authors have reached to the conclusion that IPMC materials exhibit viscoelastic behavior [9, 23], which is especially noticeable for high frequency movements [24]. However, we include the viscoelastic term in our equations by means of using Rayleigh damping [25] model, which is described for a system of one degree of freedom as follows:

$$m\frac{d^2u}{dt^2} + \xi\frac{du}{dt} + ku = f(t), \tag{4.9}$$

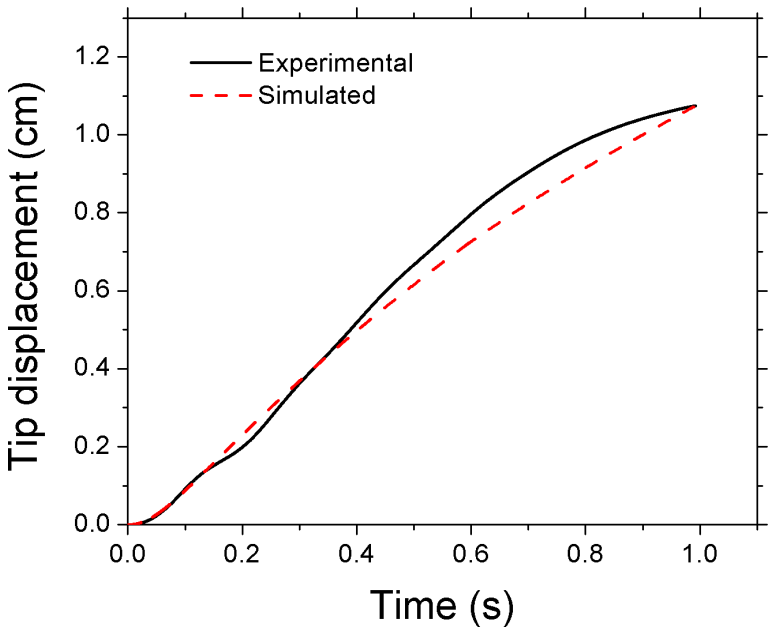

Figure 4.3: Experimental and simulation results of tip displacement. The simulation is done for potential of 2 volts. Although there is a slight difference of graphs in large displacement region, the model gives precise estimation for smaller displacement.

where the damping parameter ξ is expressed as $\xi = \alpha m + \beta k$. The parameter m is mass, k is stiffness and α and β are correspondingly damping coefficients. The equation for the multiple degrees of freedom is

$$\rho \frac{\partial^2 \vec{u}}{\partial t^2} - \nabla \cdot \left[c\nabla \vec{u} + c\beta \nabla \frac{\partial \vec{u}}{\partial t} \right] + \alpha\rho \frac{\partial \vec{u}}{\partial t} = \vec{F}. \tag{4.10}$$

By coupling Eq. (4.10) to the previously described equations, a good basic model for IPMC actuation has been obtained. The damping equation turned out to be very necessary to describe correct movement of an IPMC strip. Though the values of the parameters α and β are empirical (see Table 4.3), they have an important role of improving the dynamical behavior of the model for non-constant applied voltages.

All values, which are used in the simulations, have been brought out in Table 4.3. Fig. 4.3 shows a comparison between the simulation and an experiment [11]. More comparative figures are introduced in the next section of the paper.

Chapter 5

Self-Oscillations

5.1 Experiments

We have conducted a series of tests with IPMCs in a constant electric field in formaldehyde ($HCHO$) solution. Platinum-electroded IPMCs were prepared using the electroless deposition [26] onto Nafion 1110. The standard IPMC sample size was $0.27\,mm$ thick $\times$ $10\,mm$ wide $\times$ $50\,mm$ long. By using an INSTRONTM 5565, we measured the Young's modulus of the standard IPMC samples - $48.8\,MPa$. Actuation of the platinum electroded ionomer was carried out in a conventional electrochemical cell with three electrodes. The Reference Electrode (RE) used was a Saturated Calomel Electrode (SCE) and the two platinum electrodes functioned as the Working (WE) and Counter Electrode (CE), respectively. Voltammograms were obtained using a potentiostat/galvanostat (Radiometer Analytical, Voltalab80 Model PGZ402). Deformation data of IPMC in a cantilever configuration was obtained using a laser optical displacement sensor (Micro-Epsilon Model 1400-100). Prior to all experiments, dozens of cyclic voltammetric (CV) curves between $-0.25\,V$ and $+1.2\,V$ (vs. SCE) were performed in $0.5M\,H_2SO_4$ to confirm the absence of any residuals of impurities on the platinum surface. All experiments were performed at room temperature. Measurements show that current oscillations begin from applied potential of ca. $0.75\ V$. More information about experiments and conclusions is described in the previous paper [7].

5.2 Theoretical Background

Studies show that there are sequential electrochemical reactions, which take place on the platinum cathode. The initial burst of the current is caused by the reaction

$$CO_{ads} + OH_{ads} \rightarrow CO_2 + H^+ + e^- + 2*, \tag{5.1}$$

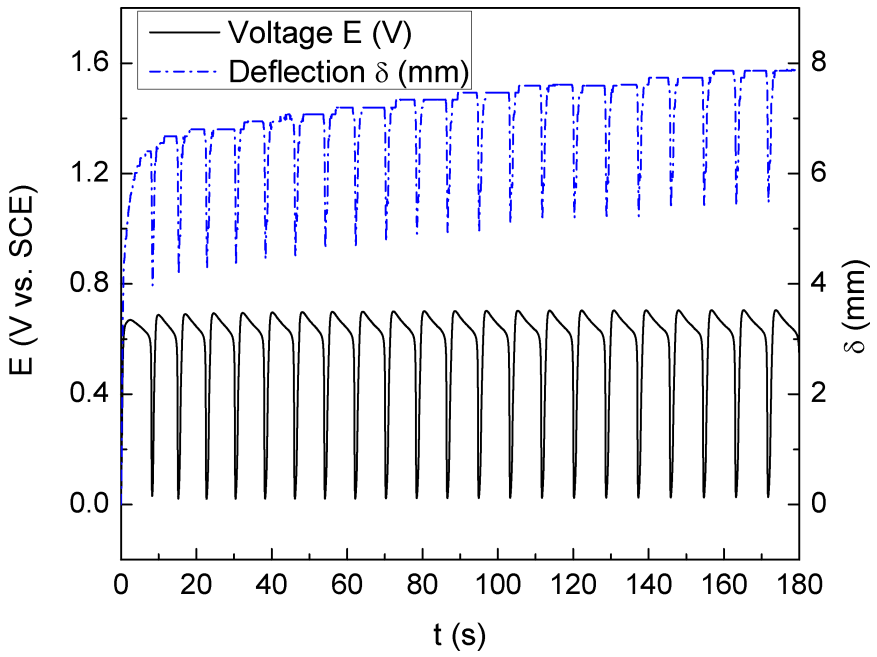

Figure 5.1: and corresponding deflection data of a platinum-IPMC in $2MHCHO + 3MH_2SO_4$ under constant current of $10mA/cm^2$ (scan rate of $1mA/s$).

where subscript *ads* denotes species adsorbed to the platinum and $*$ denotes an active platinum site. The result of the reaction (5.1) is clearing up 2 platinum sites, which causes CO to adsorb again. Due to CO poisoning, anodic current abruptly decreases until the burst again. Between current decrease and second burst, the current slightly increased due to OH adsorption. These electrochemical reactions lead to self-rhythmic motion of an IPMC as shown in Fig. 5.1. During the oxidation of formaldehyde, the intermediate (CO) of the reaction strongly binds to the platinum surface of the IPMC and blocks active sites. Since platinum is particularly vulnerable to a poisoning effect, both cathode and anode can be poisoned by CO in acidic media. In this process the resistance of platinum is increased which leads to weaker field strength between electrodes of an IPMC. Platinum also adsorbs OH which then oxidizes the CO on adjacent platinum sites to CO_2. Due to this reaction, conductivity of platinum improves and results in a stronger field strength between the electrodes. The simultaneous adsorption and desorption processes result in the oscillatory potentials which can be used as a driving source of IPMCs. Chronopotentiomentry scans show that before reaction (5.1), the following reactions occur:

$$HCHO + * \rightarrow Pt - CHO_{ads} + H^+ + e^-, \tag{5.2}$$

$$Pt - CHO \rightarrow Pt - CO_{ads} + H^+ + e^-, \tag{5.3}$$

$$H_2O + * \leftrightarrow Pt - OH_{ads} + H^+ + e^-. \tag{5.4}$$

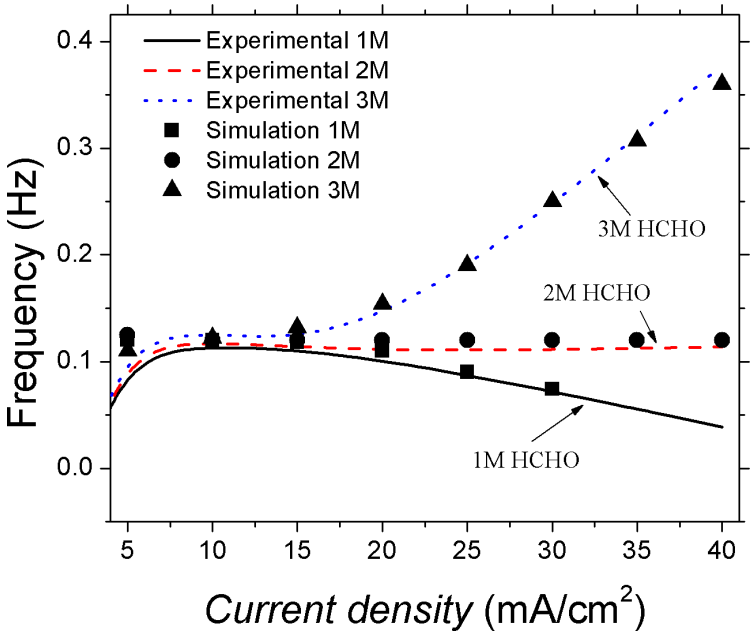

Figure 5.2: Experimental [7] and simulated frequency dependence on concentration of HCHO and applied current density. Simulations for 1 M HCHO concentration does not go past 30 mA/cm^2, because given equation system did not give reasonable results beyond that current density.

HCHO is dissociated on the electrode surface at lower anodic potentials. Higher anodic potentials cause dehydrogenation of water which results in water oxidation with intermediate Pt-OH formation. We believe that these reactions lead to oscillating potentials, which in turn lead to self-oscillating motion of the IPMC sheet.

Series of chronopotentiometry scans were conducted to characterize oscillations for different HCHO concentrations and current densities. As was brought out in our previous paper [7], the oscillations start at approximately 7 mA/cm^2. The experiments were conducted up to current density values of 40 mA/cm^2. Tests with HCHO concentrations of 1 M, 2 M, and 3 M show that oscillations frequencies remain constant up to the current density of 14 mA/cm^2, but after further increasing the current, in 1 M HCHO, the frequency decreases, in 2 M HCHO, the frequency remains constant, and in 3 M HCHO solution, the frequency starts to increase, as also shown in Fig. 5.2.

5.3 Modeling Self-Oscillations

Our goal is to develop a model for describing the frequency behavior depending on HCHO concentration and the current density. The basic model and concepts are introduced by D. Kim [19] and work of P. Strasser [20]. To describe the oscillations, four dynamic parameters, therefore four differential equations, must be observed: concentration of adsorbed OH, CO, the change of

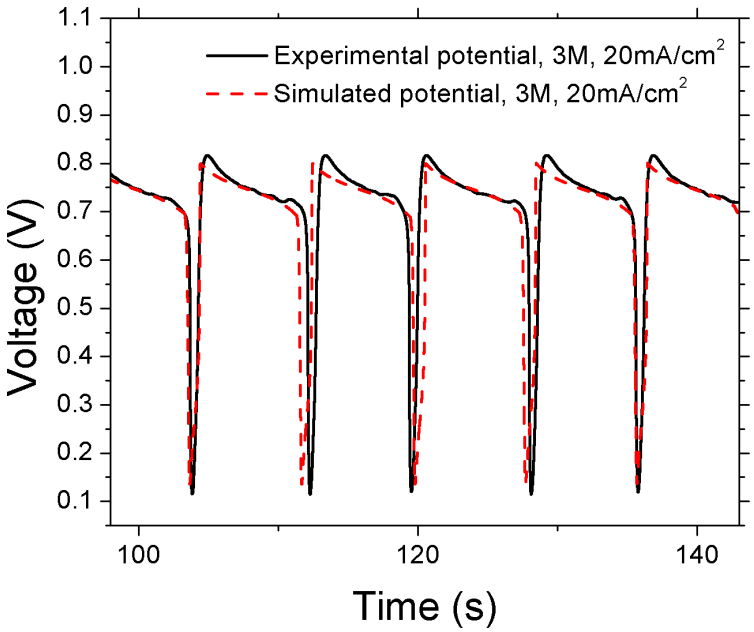

Figure 5.3: Potential oscillations. Measured data [19] and simulated data for 3 M HCHO solution. The potential oscillations were measured between the cathode and anode of the IPMC strip during the experiment. The applied current was maintained at constant value of 20 mA/cm^2.

the double layer potential due to electrochemical reactions, and the change of the concentration of $HCHO$ near the surface of platinum. First two variables are expressed for a certain current density and $HCHO$ concentration as [19]:

$$\dot{\theta}_{CO} = k_2 M - k_4 \theta_{CO} \theta_{OH}, \tag{5.5}$$

$$\dot{\theta}_{OH} = k_3 \theta_{CO} M - k_{-3} \theta_{OH} - k_4 \theta_{CO} \theta_{OH}, \tag{5.6}$$

where θ_{CO} and θ_{OH} are normed adsorption coverages of CO and OH. Variables k_i and M are described by equations

$$k_i(\phi) = exp\left[s_i(\phi - \phi_i)\right], \tag{5.7}$$

$$M = (1 - \theta_{CO} - \theta_{OH}), \tag{5.8}$$

where s_i are modeling coefficients and ϕ_i are potentials of the reactions [19]. As our model is highly dynamic, the double layer with thickness δ near the platinum electrode is introduced. At the far end of the layer, the concentration of the formic acid is considered constant, and due to the adsorption of $HCHO$ on Pt, the concentration of the solution is changing in time near the electrode. There are two components responsible of decrease of the concentration. The first one is direct oxidation of the formic acid to CO_2 and $2H^+$, the second one is adsorption of CO on

the platinum surface due to electrochemical reactions [20]. The mechanism, which restores the $HCHO$ concentration near the surface is diffusion. So the amount of the formic acid is decreasing significantly while the adsorption rate is high and increasing due to the diffusion during the low adsorption period. The equation describing the diffusion process is

$$\frac{\partial c_{FA}}{\partial t} = \nabla \cdot (D_{FA} \nabla c_{FA}) \tag{5.9}$$

with constant concentration at the far end of the double layer and flux

$$f = k_2 M \left(1 + k c_r\right) S_{tot}, \tag{5.10}$$

as boundary condition on the electrode. Here S_{tot} denotes the total number of platinum sites per surface area, c_r is normed concentration near boundary layer and equals $c_r = c_{FA}/c_0$, where c_0 is an initial concentration. Variable k is a simulation constant. The second term of Eq. (5.10) represents simplified version of the direct oxidation path [20]. Considering those equations and interesting nature of frequency characteristic for different amounts of HCHO (Fig. 5.2), we can now describe empirical, gray box [27] equation for the last dynamic variable - the double layer potential:

$$\begin{aligned} \dot{\phi} \quad = \quad & \frac{1}{C_{dl}} \left[j_{th} - j_d + A \; B \; j^2 \; \left(j - j_{th}\right) c_r - \right. \\ & \left. - S_{tot} F \left(k_1 M + k_4 \theta_{CO} \theta_{OH}\right) \right], \end{aligned} \tag{5.11}$$

where j is applied current density, j_{th} is threshold current density with approximate value of 10 mA/cm^2, j_d is direct current density and is proportional to the second term of Eq. (5.10). The variable B is explicitly written as $B = c_0 - c_{neutral}$, where $c_{neutral}$ corresponds to concentration of 2 M. This is denoted as "natural" concentration, because as it is shown in Figure 5.2, the oscillation frequency for the case $c_0 = c_{neutral} = 2\ M$ does not depend on the applied current density. The numeric data can be found in Table 5.1. The third term in Eq. (5.11) is empirical and reflects the interesting behavior of the oscillations frequency for different formic acid concentrations. Other terms are similar to the ones described by Strasser [20]. However, some values are adjusted to get realistic simulation results. Measured voltage oscillation comparison to simulation data could be seen in Fig. 5.3. The simulation does not require any change in boundary or inital conditions for the basic model, which is described in the previous chapter. However, equations (5.5), (5.6), (5.7), and (5.11) are simulated using the weak form differential equation on the anode boundary.

5.4 Modeling Results

By using the obtained voltage output in the base Finite Element Model, which is described in the previous chapter, we can simulate oscillating deflection of an IPMC muscle. As it is shown in Fig. 5.2, the model is quite flexible, i.e parameters such as HCHO concentration and current

Table 5.1: Variables and values used in the simulation of electrochemical oscillations.

Parameter	Value	Unit
S_{tot}	0.5×10^{-6}	mol/cm^2
C_{dl}	1	mF/cm^2
A	1.2	$cm^7/\left(mA^2 \times mol\right)$
k	100	-
δ^1	3×10^{-2}	cm
${D_{FA}}^1$	2.5×10^{-5}	cm^2/s
${\phi_{1,2,3,-3,4}}^2$	[0.2, 0.3, 0.01, 0.512, 0.77]	V
${s_{1,2,3,-3,4}}^2$	[10, −11, 9, −9, 20]	V^{-1}

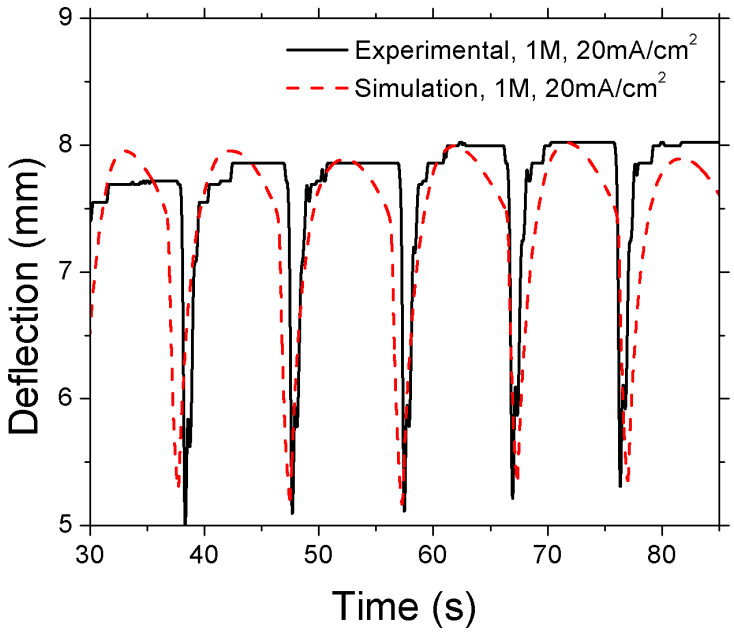

Figure 5.4: Oscillating tip displacement. Experimental [19] data and simulation data for 1 M HCHO solution, applied current density of 20 mA/cm^2.

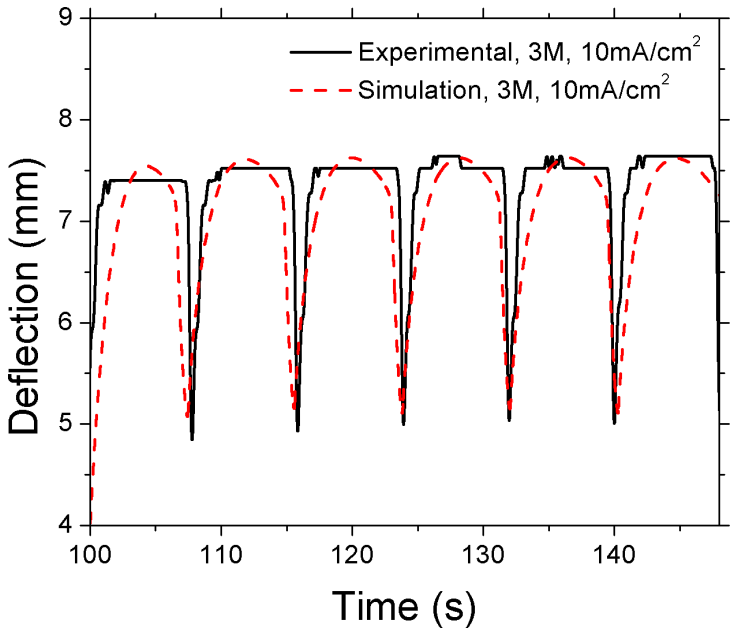

Figure 5.5: Oscillating tip displacement. Experimental [19] data and simulation data for 3 M HCHO solution, applied current density of 10 mA/cm^2.

density could be changed without loss of model's accuracy. Also the measured voltage and modeled voltage is in very good accordance with modeling results (Fig. 5.3).

Two sample results for different HCHO concentrations and current densities are shown in Figures 5.4 and 5.5. As it could be seen, the amplitude, frequency and for the most part, shape of the deflection show reasonable agreement between modeling and experimental data. However, there is some disharmony at the areas of maximum deflection, where the experiments show distinctly sharp deflections in comparison to rather smooth simulation results. This will be studied further in future.

Chapter 6

Summary and Conclusions

We have developed a Finite Element model for simulating actuation of an IPMC. The model is largely based on physical quantities and well known or measurable variables. The migration and diffusion of the counter ions inside the Nafion^{TM} polymer is described along the electric field change due to the charge imbalance. This in turn is tied into continuum mechanics and dynamics equations, forming a complete system of equations to describe the bending of an IPMC sheet.

The comparison of experimental and simulated tip displacement in time shows reasonable agreement, especially for smaller deflections. The future work is to perform simulations more precise for large displacements, possibly including equations, which describe voltage distribution on the surface of the electrodes depending on the curvature of the IPMC. Taking into account the surrounding environment of the IPMC could also improve the results.

The second part of the work describes the extended model for self-oscillating IPMCs. The oscillations occur when a platinum coated IPMC is immersed into formic acid solution and subjected to a constant potential or current. The extended model takes into account formic acid concentration changes near the electrode and poisoning level of the platinum sites. This in turn results in the oscillating double layer potential, which is used in the base model for calculating time dependent tip displacement of the IPMC muscle. For the most part, the model follows simulation data closely. However, the experimental deflection shows distinctly sharp movements at certain regions, but the simulation gives rather smooth displacement profiles. The future work includes studying further this interesting behavior and possibly improving the model.

We want to acknowledge the support of the US Office of Naval Research (N00014-04-0673) and Estonian Science Foundation grant #6763. Also we acknowledge Estonian Archimedes Foundation for travel support of Deivid Pugal to University of Nevada, Reno.

References

[1] M. Shahinpoor and K. J. Kim, "Ionic polymer-metal composites: I. fundamentals," *Smart Materials and Structures* **10**, pp. 819–833, Aug. 2001.

[2] Q. Zhang, V. Bharti, and X. Zhao, "Giant Electrostriction and Relaxor Ferroelectric Behavior in Electron-Irradiated Poly (vinylidene fluoride-trifluoroethylene) Copolymer," *Science* **280**(5372), p. 2101, 1998.

[3] E. 1 Smela, "Conjugated polymer micromuscles," *MST News* , pp. 16–18, Sept. 2003.

[4] R. H. Baughman, C. Cui, A. A. Zakhidov, Z. Iqbal, J. N. Barisci, G. M. Spinks, G. G. Wallace, A. Mazzoldi, D. De Rossi, A. G. Rinzler, O. Jaschinski, S. Roth, and M. Kertesz, "Carbon nanotube actuators," *Science* **284**, pp. 1340–4, May 21.

[5] R. Pelrine, R. Kornbluh, Q. Pei, and J. Joseph, "High-speed electrically actuated elastomers with strain greater than 100%," *Science* **287**, pp. 836–9, Feb. 4.

[6] S. J. Kim, G. M. Spinks, S. Prosser, P. G. Whitten, G. G. Wallace, and S. I. Kim, "Surprising shrinkage of expanding gels under an external load," *Nature Materials* **5**, pp. 48–51, Jan. 2006.

[7] D. Kim, K. J. Kim, Y. Tak, D. Pugal, and I.-S. Park, "Self-oscillating electroactive polymer actuator," *Applied Physics Letters* **90**(18), p. 184104, 2007.

[8] D. Pugal, K. J. Kim, A. Punning, H. Kasemagi, M. Kruusmaa, and A. Aabloo, "A self-oscillating ionic polymer-metal composite bending actuator," *Journal of Applied Physics* **103**(8), p. 084908, 2008.

[9] K. M. Newbury and D. J. Leo, "Linear electromechanical model of ionic polymer transducers - part i: Model development," *Journal of Intelligent Material Systems and Structures* **14**, pp. 333–342, June 2003.

[10] K. Jung, J. Nam, and H. Choi, "Investigations on actuation characteristics of IPMC artificial muscle actuator," *Sensors and Actuators A (Physical)* **107**, pp. 183–92, Oct. 15.

[11] A. Punning, M. Kruusmaa, and A. Aabloo, "Surface resistance experiments with IPMC sensors and actuators," *Sensors and Actuators, A: Physical* **133**, pp. 200–209, Jan. 2007.

[12] T. Wallmersperger, B. Kroplin, and R. W. Gulch, "Coupled chemo-electro-mechanical formulation for ionic polymer gels - numerical and experimental investigations," *Mechanics of Materials* **36**, pp. 411–420, May 2004.

[13] S. Nemat-Nasser and S. Zamani, "Modeling of electrochemomechanical response of ionic polymer-metal composites with various solvents," *Journal of Applied Physics* **100**(6), p. 064310, 2006.

[14] Y. Toi and S.-S. Kang, "Finite element analysis of two-dimensional electrochemical-mechanical response of ionic conducting polymer-metal composite beams," *Computers and Structures* **83**, pp. 2573–2583, Dec. 2005.

[15] S. Lee, H. C. Park, and K. J. Kim, "Equivalent modeling for ionic polymer - metal composite actuators based on beam theories," *Smart Materials and Structures* **14**, pp. 1363–1368, Dec. 2005.

[16] T. Wallmersperger, D. J. Leo, and C. S. Kothera, "Transport modeling in ionomeric polymer transducers and its relationship to electromechanical coupling," *Journal of Applied Physics* **101**(2), p. 024912, 2007.

[17] B. Miller and A. Chen, "Oscillatory instabilities during the electrochemical oxidation of sulfide on a pt electrode," *Journal of Electroanalytical Chemistry* **588**, pp. 314–323, Mar. 2006.

[18] K. Krischer, "Spontaneous formation of spatiotemporal patterns at the electrode | electrolyte interface," *Journal of Electroanalytical Chemistry* **501**, pp. 1–21, Mar. 2001.

[19] D. Kim, *Electrochemically Controllable Biomimetic Actuator*. PhD thesis, University of Nevada, Reno, USA, 2006.

[20] P. Strasser, M. Eiswirth, and G. Ertl, "Oscillatory instabilities during formic acid oxidation on pt(100), pt(110) and pt(111) under potentiostatic control. II. model calculations," *Journal of Chemical Physics* **107**, July 1997.

[21] S. Nemat-Nasser and Y. Wu, "Comparative experimental study of ionic polymer-metal composites with different backbone ionomers and in various cation forms," *Journal of Applied Physics* **93**, pp. 5255–5267, May 2003.

[22] S. Nemat-Nasser and J. Y. Li, "Electromechanical response of ionic polymer-metal composites," *Journal of Applied Physics* **87**, Apr. 2000.

[23] K. Yagasaki and H. Tamagawa, "Experimental estimate of viscoelastic properties for ionic polymer-metal composites," *Physical Review E - Statistical, Nonlinear, and Soft Matter Physics* **70**, pp. 052801–1, Nov. 2004.

[24] K. M. Newbury and D. J. Leo, "Linear electromechanical model of ionic polymer transducers - part II: Experimental validation," *Journal of Intelligent Material Systems and Structures* **14**, pp. 343–358, June 2003.

[25] R. Lord, "The Theory of Sound," *New York, Dover* **2**, p. 226, 1945.

[26] K. Kim and M. Shahinpoor, "Ionic polymer-metal composites: II. Manufacturing techniques.," *Smart Materials and Structures* **12**(1), pp. 65–79, 2003.

[27] M. Shahinpoor and K. J. Kim, "Ionic polymer-metal composites: III. modeling and simulation as biomimetic sensors, actuators, transducers, and artificial muscles," *Smart Materials and Structures* **13**, pp. 1362–1388, Dec. 2004.

Ostsilleeruva IPMC Aktuaatori Mudel

Deivid Pugal

Kokkuvõte

Käesolevas töös on koostatud IPMC tüüpi materjalide mudel. IPMC on üks paljudest elektroaktiivsetest polümeeridest nagu ferroelektrilised polümeerid, juhtivad polümeerid, dielektrilised elastomeerid ja ioonpolümeer geelid. Kõik need materjalid on väärtuslikud paljudes rakendustes mikrorobootikast kosmosetehnoloogiateni. Seda liiki materjalide eeliseks on kergus, hääletu töö ja suur paindeulatus. Mitmed elektroaktiivsed polümeerid nagu IPMC on võimelised toimima ka märjas keskonnas. Neid omadusi silmas pidades võib kõiki eelnimetatud materjale kutsuda n.ö kunstlihasteks.

Käesolevas töös on koostatud IPMC tüüpi materjali jaoks füüsikaline mudel Lõplike Elementide Meetodit (LEM) kasutades. Mudel koosneb kahest komponendist: üks ja põhiline on baasmudel, mille abil on võimalik simuleerida lihtsat IPMC materjali paindumist. See komponent sisaldab endas IPMC sees toimuvaid põhilis protsesse (nagu ioonide liikumine, elektrivälja kirjeldus) kirjeldavaid võrrandeid. Teine osa mudelist keskendub elektrokeemiliste protsesside kirjeldamisele ning see võimaldab simuleerida iseostsilleeruvat IPMC materjali. Nimelt oleme teinud arvukalt teste IPMC matejalidega, mis on kastetud $HCHO$ lahusesse. Rakendades materjalile konstantse pinge, alates $0.75V$, saab mõõta voolu ja ka materjali enda võnkumisi. Seega mudeli teine osa ongi baasmudeli üks võimalik laiendus, mille abil saame modelleerida reaalset füüsikaliselt huvipakkuvat probleemi.

Baasmudeli võrrandid kirjeldavad mitut erinevat füüsikalist domeeni. Nernst Planck'i võrrand kirjeldab ioonide liikumist, Gaussi võrrand kirjeldab elektrivälja IPMC materjalis ja mitmesugused pideva keskkonna mehhaanika võrrandid ($\sigma - \varepsilon$ seosed) kirjeldavad materjali paindumist. Mudeliga sooritatud arvutuste ja katseandmete võrdlemine näitab head kooskõla.

Mudeli teine osa on sisuliselt baasmudeli laiendus elekrokeemiliste ostsillatsioonide kirjeldamiseks. See koosneb neljast süsteemi pandud ajast sõltuvast differentsiaalvõrrandist, mis kirjel-

davad mitmesuguseid elektrokeemilis protsesse plaattina katoodi pinnal. Võrrandite muutujateks on $HCHO$ kontsentratsiooni katoodi lähedal, CO ja OH adsorbatsioon ajas ja kaksikkihi potentsiaali muutumine ajas. Need võrrandid on samuti koostatud käesoleva töö raames.

Võrreldes nii baasmudeli kui ka laiendatud mudeli abil arvutatud IPMC tüüpi materjalide paindumist elektriväljas, näeme väga head kooskõla eksperimendiga. Siiski eksperiment $HCHO$ lahuses asetseva kunstlihasega näitab mõningaid järske liikumisi erinevalt meie mudelist. Selle huvitava käitumise uurinime on edaspidise uurimsitöö osa.

Käesolevas töös esitatud tulemused on ka avaldatud ajakirjades Applied Physics Letters [7] ja Journal of Applied Physics [8].

Publications

I - Applied Physics Letters

Self-oscillating electroactive polymer actuator

Doyeon Kim and Kwang J. Kim[a)]
Active Materials and Processing Laboratory, Mechanical Engineering Department, University of Nevada, Reno, Nevada 89557

Yongsuk Tak
School of Chemical Engineering, Inha University, Inchon, Kyoungki Do 402-751, South Korea

Deivid Pugal
Active Materials and Processing Laboratory, Mechanical Engineering Department, University of Nevada, Reno, Nevada 89557 and IMS Laboratory, Institute of Technology, Tartu University 50410, Estonia

Il-Seok Park
Active Materials and Processing Laboratory, Mechanical Engineering Department, University of Nevada, Reno, Nevada 89557

(Received 9 December 2006; accepted 9 April 2007; published online 2 May 2007)

To drive the electroactive polymer (EAP) materials and subsequently control their strain generation, the need for power electronics and driving circuits has been eminent. In this letter the authors demonstrate a spontaneous actuation of an electroactive polymer that requires only dc power to produce its ac responses. Such a dc-to-ac response of the EAP was achieved by the deposition of an effective electrocatalyst, i.e., platinum, on an ionomer, Nafion™. The coated ionomer was immersed into an acidic formaldehyde solution. An applied dc voltage will produce current oscillations in the system, and therefore oscillating bending of the actuator. © *2007 American Institute of Physics*. [DOI: 10.1063/1.2735931]

A number of representative electroactive polymeric materials of interest include ferroelectric polymers,[1] conducting polymers,[2] ionomeric polymer-metal composites[3] (the subject of this study), carbon nanotubes,[4] dielectric elastomers,[5] and ionic polymeric gels.[6] These materials exhibit an active deformation capability under applied voltages, producing useful force density. Ionomers (such as a perfluorinated sulfonic acid polymer, i.e., Nafion™) in a composite form with a conductive metallic medium such as platinum (Pt) are called ionic polymer-metal composites (IPMC). In a cantilever configuration, these materials can exhibit large dynamic deformation if placed in a time-varying low electric field of less than a few volts.

Spontaneous oscillations are a widespread phenomenon in nature. They have been studied for large number of experiments, including electrochemical systems, such as the oxidation of metals and organic materials.[7] Electrochemical systems exhibiting instabilities often behave like activator-inhibitor systems. In these systems the electrode potential is an essential variable and takes on the role either of the activator or of the inhibitor. If certain conditions are met, an activator-inhibitor system can generate oscillations.[8]

Platinum-electroded IPMCs were prepared using the electroless deposition[9] onto Nafion 1110. The standard IPMC sample size was 0.27 mm thick by 10 mm wide by 50 mm long. By using an INSTRON™ 5565, we measured Young's modulus of the standard IPMC samples—48.8 MPa.

Actuation of the platinum-electroded ionomer was carried out in a conventional electrochemical cell with three electrodes. The reference electrode used was a saturated calomel electrode (SCE) and the two platinum electrodes functioned as the working and counterelectrode, respectively. Voltammograms were obtained using a potentiostat/galvanostat (Radiometer Analytical, Voltalab80 model PGZ402). Deformation data of IPMC in a cantilever configuration were obtained using a laser optical displacement sensor (Micro-Epsilon Model 1400-100). Prior to all experiments, dozens of cyclic voltammetric curves between −0.25 and +1.2 V (versus SCE) were performed in 0.5*M* H_2SO_4 to confirm the absence of any residuals of impurities on the platinum surface. All experiments were performed at room temperature.

We conducted a series of tests with IPMCs in formaldehyde (HCHO) solutions. Measurements under constant electric field showed that current oscillations occur from onset potential of approximation 0.75 V. The initial burst of current at this voltage is due to the reaction $CO_{ads}+OH_{ads} \rightarrow CO_2+H^+ + e^- + 2^*$, where subscript ads denote species adsorbed on the surface of platinum and * denotes an active platinum site. This reaction frees up two platinum sites, which cause CO again to adsorb on the surface. Due to CO poisoning, anodic current abruptly decreases until the burst again. Between current decrease and second burst, the current slightly increased due to OH adsorption. These electrochemical reactions lead to self-rhythmic motion of an IPMC, as shown in Fig. 1.

During the oxidation of formaldehyde, the intermediate (CO) of the reaction strongly binds to the platinum surface of the IPMC and blocks active sites. Since platinum is particularly vulnerable to a poisoning effect, both cathode and anode can be poisoned by CO in acidic media. In this process the resistance of platinum is increased, which leads to weaker field strength between electrodes of an IPMC. Platinum also adsorbs OH which then oxidizes the CO on adjacent platinum sites to CO_2. Due to this reaction, conductivity of platinum improves and results in a stronger field strength between the electrodes. The simultaneous adsorption and de-

[a)]Electronic mail: kwangkim@unr.edu

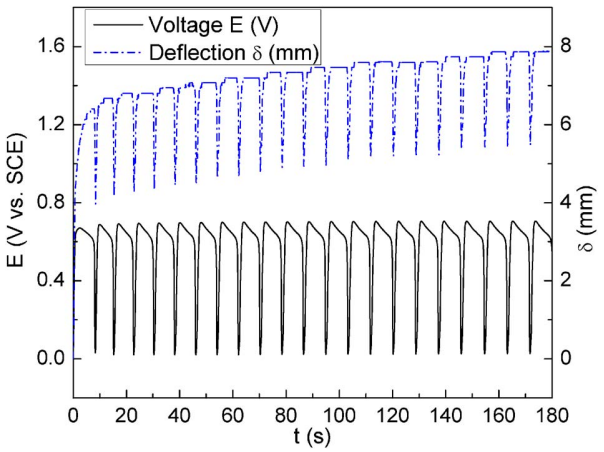

FIG. 1. (Color online) Chronopotentiogram and corresponding deflection data of a platinum IPMC in 2*M* HCHO+3*M* H_2SO_4 under constant current of 10 mA/cm^2 (scan rate of 1 mA/s).

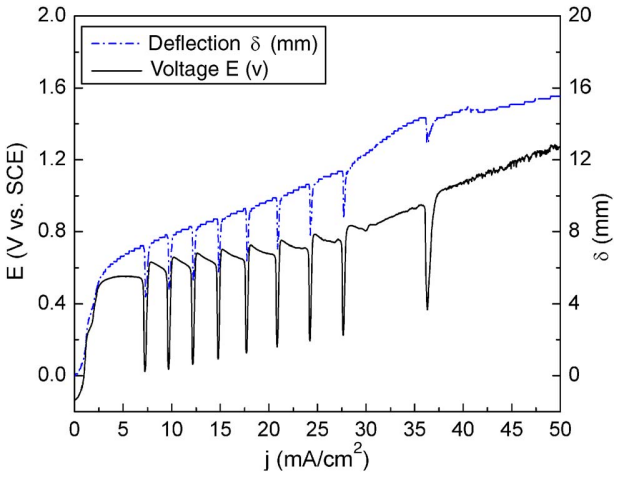

FIG. 2. (Color online) Galvanostatic linear sweep voltammograms of a platinum IPMC in 1*M* HCHO+3*M* H_2SO_4 at the scan rate of 1 mA/s.

sorption processes result in the oscillatory potentials which can be used as a driving source of IPMCs.

Chronopotentiometry scans for three different concentrations of HCHO help us to characterize behavior of IPMC in HCHO solution. For all cases, oscillations start at approximately 7 mA/cm^2 (further noted as threshold current) with a constant value of 0.11–0.13 Hz up to the current density of 14 mA/cm^2. After further increasing current, in 1*M* HCHO, the frequency decreases as shown in Fig. 2. In 2*M* HCHO, the frequency maintains a constant value regardless of higher current density, and in 3*M* HCHO, the frequency increases. Tests also show that maximum potential difference increases until threshold current and stays constant after that. However, maximum deflection tends to decrease after increasing current over threshold current. We achieved the largest deflection of 2.86 mm at 10 mA/cm^2 in 1*M* HCHO. It is interesting to note that relationship between corresponding deflection and potential on the electrode is nearly linear. So, by varying concentration of HCHO and changing driving current, it is possible to create self-oscillating IPMC systems with different characteristics, as shown in Fig. 3, appropriate for specific tasks.

Electrochemical oscillations during electro-oxidation of small organic molecules under specific conditions are usually observed. It was reported that HCHOOH shows electrochemical oscillation phenomena during oxidation.[10] As we have seen, oscillations obtained from a HCHO system can be useful for self-oscillatory IPMC systems. However, cyclic voltammetry tests were conducted for HCHOOH and in addition, for alcohols, such as CH_3OH, C_2H_5OH, and C_3H_7OH to find out a possibility of using them in IPMC systems. We found that there are no peaks in alcohol solutions from 0 to 1.4 V. It is determined that adsorbed CO coming from those organic molecules converts into CO_2 without oscillation phenomena. There are oscillations in HCOOH solution. However, peaks are shown in a narrower range of applied current and the number of oscillations is also much smaller than in the HCHO system. This means that HCOOH is not proper for a self-oscillatory IPMC with high frequency. It could be used for low-frequency oscillations. However, alcohol solutions do not work at all.

Biological systems usually exhibit rhythmic phenomena. Their typical time scale is in the range from less than a second to years. How can this effect be really important for

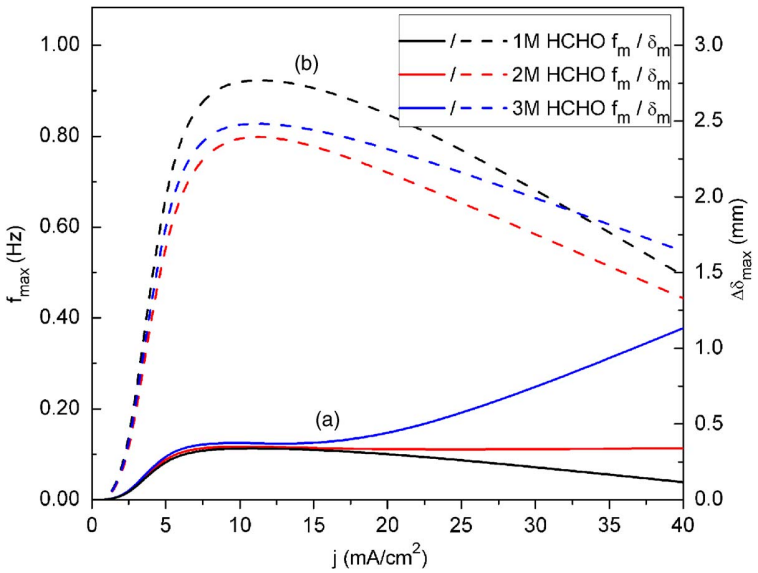

FIG. 3. (Color online) Current dependence (a) of oscillation frequency of the platinum IPMC and maximum deflection difference (b) of the oscillations with three different concentrations of HCHO (scan rate of 1 mA/s).

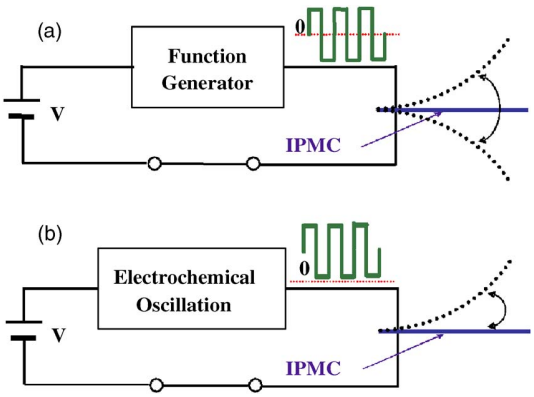

FIG. 4. (Color online) Illustration of conventional (a) and self-oscillatory (b) operations of IPMC-based artificial muscles.

developing IPMC based applications? The self-oscillatory operation allows simplifying the driving electronics of IPMC systems and can lead to significant increase of the payload. It can also be useful as a means of minimizing the use of complex electronics in many engineering applications (see Fig. 4). We have been able to achieve frequencies in the range of 0–1 Hz and deflections up to almost 3 mm. If further developed, the self-oscillatory feature of IPMC allows one to obtain desired properties for numerous future engineering applications. Potential applications include self-oscillating propulsor blades for small underwater vehicles, self regulating drug delivery systems, artificial organs such as heart, biosensors, etc.

Authors from University of Nevada, Reno acknowledge the financial support from the U.S. Office of Naval Research (Award No: N00014-04-0673). The author from Tartu University acknowledges financial support from Estonian Science Foundation, ETF Grant No. 6763. The authors also thank the partial financial support from Archimedes Foundation in Estonia for the travel support of Deivid Pugal to the University of Nevada, Reno.

[1]Q. M. Zhang, V. Bharti, and X. Zhao, Science **280**, 2101 (1998).
[2]E. Smela, Adv. Mater. (Weinheim, Ger.) **15**, 481 (2003).
[3]M. Shahinpoor and K. J. Kim, Smart Mater. Struct. **10**, 819 (2001).
[4]R. H. Baughman, C. Cui, A. A. Zakhidov, Z. Iqbal, J. N. Barisci, G. M. Spinks, G. G. Wallace, A. Mazzoldi, D. De Rossi, A. G. Rinzler, O. Jaschinski, S. Roth, and M. Kertesz, Science **284**, 1340 (1999).
[5]R. Pelrine, R. Kornbluh, Q. Pei, and J. Joseph, Science **287**, 836 (2000).
[6]S. Kim, G. Spinks, S. Prosser, P. Whitten, G. Wallace, and S. Kim, Nat. Mater. **5**, 48 (2006).
[7]B. Miller and A. Chen, J. Electroanal. Chem. **588**, 314 (2006).
[8]K. Krischer, J. Electroanal. Chem. **501**, 1 (2001).
[9]K. J. Kim and M. Shahinpoor, Smart Mater. Struct. **12**, 65 (2003).
[10]T. J. Schmidt, B. N. Grgur, N. M. Markovic, and P. N. J. Ross, J. Electroanal. Chem. **500**, 36 (2001).

II - Journal of Applied Physics

A self-oscillating ionic polymer-metal composite bending actuator

Deivid Pugal,[1,2,a)] Kwang J. Kim,[1,b)] Andres Punning,[2] Heiki Kasemägi,[2] Maarja Kruusmaa,[2] and Alvo Aabloo[2]
[1]*Active Materials and Processing Laboratory, Mechanical Engineering Department, University of Nevada, Reno, Nevada 89557, USA*
[2]*IMS Lab, Institute of Technology, Tartu University, Tartu 50411, Estonia*

(Received 12 June 2007; accepted 4 February 2008; published online 25 April 2008)

This paper presents an electromechanical model of an ionic polymer-metal composite (IPMC) material. The modeling technique is a finite element method (FEM). An applied electric field causes the drift of counterions (e.g., Na^+), which, in turn, drags water molecules. The mass and charge imbalance inside the polymer is the main cause of the bending motion of the IPMC. The studied physical effects have been considered as time dependent and modeled with FEM. The model takes into account the mechanical properties of the Nafion polymer as well as the thin coating of the platinum electrodes and the platinum diffusion layer. The modeling of the electrochemical reactions, in connection with the self-oscillating behavior of an IPMC, is also considered. Reactions occurring on the surface of the platinum electrode, which is immersed into formaldehyde (HCHO) solution during the testing, are described using partial differential equations and also modeled using FEM. By coupling the equations with the rest of the model, we are able to simulate the self-oscillating behavior of an IPMC sheet. © *2008 American Institute of Physics*. [DOI: 10.1063/1.2903478]

I. INTRODUCTION

Electroactive polymer (EAP) based materials are valuable for many applications, from microrobotics to military and space applications. Some of the advantages of EAP materials are their light weight, noiseless actuation, simple mechanics, and large displacement capabilities. In addition, some EAPs, such as ionic polymer-metal composites (IPMCs),[1] are able to function in aqueous environments. These qualities make the materials applicable in creating artificial muscles. In this paper, we consider simulations of the IPMC type materials using the finite element method (FEM).

IPMC materials are highly porous polymer materials, such as Nafion™, and are filled with an ion-conductive liquid. Some IPMCs are water based, operating in an aquatic environment where the current is caused by ions such as Na(+) and K(+) being dissociated in water. Another kind of IPMCs—ionic liquid based—does not need a wet environment to function. A sheet of an ionic polymer is coated with a thin metal layer, usually platinum or gold. All free, mobile cations inside the polymer migrate towards an electrode due to an applied electric field, causing an expansion of the material on one side of the sheet and contraction on the other side, resulting in the bending of the sheet.

In order to simulate the actuation of an IPMC sheet, we need to solve coupled problems, which will be difficult due to the complex nature of the bending. The simulations take place in different domains such as mechanical, electrostatic and mass transfer, and even electrochemical for more advanced models. Some authors[2,3] have already simulated mass transfer and electrostatic effects, and we used similar approaches in our model. Toi and Kang showed a FEM including the viscosity terms during the transportation processes.[4] The basis of this described model is a rectangular beam with two pairs of electrodes. Our approach to simulating mechanical bending is to take advantage of the numerical nature of FEM problems—to use continuum mechanics equations instead of the more commonly used analytical equations.[5,6] By coupling equations from different domains, we get a model of an IPMC muscle sheet, which allows us to use it as a starting point for solving more complex problems; thus, we have introduced a simulation of electrochemical reactions using a platinum electrode of an IPMC sheet, leading to a self-oscillating actuation. Spontaneous oscillations are common phenomena in nature, including electrochemical systems such as oxidation of organic materials and metals.[7] Under certain conditions, such systems can generate oscillations.[8] We have conducted a series of tests, where an IPMC sheet has been immersed into an acidic formaldehyde (HCHO) solution and exposed to a constant potential. The measurements, however, show current oscillations, which, in turn, result in an oscillating bending of the IPMC sheet.[9] Hence, we have introduced a FEM model in this paper to describe the time-dependent bending of a self-oscillating IPMC.

II. BENDING SIMULATION DETAILS

An IPMC sheet consists of a polymer host and a metal coating. In our experiments, we used Nafion™ 117 that was coated with a thin layer of platinum. Mass transfer and electrostatic simulations were performed in three mechanical domains—pure backbone polymer, pure platinum coating, and a mixture of polymer and platinum. Some platinum diffuse into the polymer host during the coating process.[10] The physical properties and dimensions of a pure 2-μm-thick platinum coating are considered only when calculating the

a)Electronic mail: david@ut.ee.
b)Electronic mail: kwangkim@unr.edu.

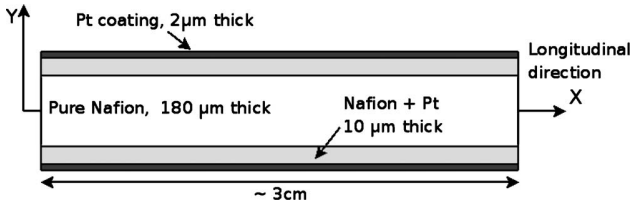

FIG. 1. Illustration of domains and dimensions used in simulations. The length of 3 cm was used also in a number of experiments. Note that there are three different mechanical domains—pure Nafion™ polymer, pure Pt coating, and a diffusion layer where Pt has diffused into the polymer.

bending. These tests give us five mechanical domains as shown in Fig. 1. Most simulations are carried out on an IPMC strip, 2–4 cm long, with a 200-μm-thick polymer, including a 10-μm-thick Pt diffusion region on each side, and coated with 2-μm-thick platinum, in a cantilever configuration. One end of the strip is fixed.

The Nernst–Planck equation describes diffusion, convection, and, in the presence of an electric field and charges, migration of the particles. The general form of the equation is

$$\frac{\partial C}{\partial t} + \nabla(-D\nabla C - z\mu FC\nabla\Phi) = -\mathbf{u}\cdot\nabla C, \tag{1}$$

where C is the concentration, D the diffusion constant, F the Faraday constant, $\mathbf{u}$ the velocity, z the charge number, ϕ the electric potential, and μ the mobility of species. The mobility of the species is found using the known relation $\mu = D/RT$, where T is the absolute temperature and R is the universal gas constant. Movable counterions are described by Eq. (1). As the anions are fixed, they maintain a constant charge density throughout the polymer. After a voltage is applied to the electrodes of an IPMC, all free cations start migrating towards the cathode, causing a current in the outer electric circuit. Due to the fact that ions cannot move beyond the boundary of the polymer, charges start accumulating, resulting in an increase in the electric field, which cancels out the applied field. The process could be described by Gauss law as follows:

$$\nabla\cdot\mathbf{E} = -\Delta\Phi = \frac{F\cdot\rho_c}{\varepsilon}, \tag{2}$$

where ρ_c is the charge density, c is the absolute dielectric constant, and E is the strength of the electric field. The charge density variable is related to charge concentration as follows:

$$\rho_c = zC + z_{\text{anion}}C_{\text{anion}}. \tag{3}$$

The second term in Eq. (3) is constant at every point of the polymer. The coupling between Eqs. (1) and (2) is strong, i.e., no weak constraints were used. The absolute dielectric constant ε could be explicitly written as $\varepsilon = \varepsilon_0\varepsilon_r$, where ε_0 is the dielectric constant in vacuum and is equal to 8.85×10^{-12} F/m. The measured value of the absolute dielectric constant ε is shown in Table I. A steady state of the cations forms when the electric field, created by distribution of cations, cancels out the applied electric field. The strength of the electric field inside the polymer is approximately zero, as

TABLE I. Parameter values used in bending simulations.

Parameter	Value	Unit
D	1×10^{-5}	cm^2/s
R	8.31	l/(K mol)
T	293	K
z	1	⋯
F	96.5×10^6	mC/mol
ϵ	25	mF/m
G	110	K m/mol
H	10	$\text{N m}^4/\text{mol}^2$
α_{polymer}	0	s^{-1}
β_{polymer}	1.5	s

shown in Fig. 2. The steady state cation concentration, with the average value of 1200 mol/m^3, is also shown in the same figure. It is interesting to note that there are fluctuations in charge distribution only in thin boundary layers, leading to the conclusion that there is no charge imbalance inside the polymer. The general understanding is that the locally generated charge imbalance near the platinum electrodes is directly connected to—and mainly responsible for—the bending of an IPMC.[11] Therefore, we define the longitudinal force per unit area at each point in the polymer of an IPMC as follows:[6]

$$\mathbf{F} = (G\rho_c + H\rho_c^2)\hat{x}, \tag{4}$$

where ρ_z is the charge density, and G and H are constants found by fitting simulations, according to experimental results, using system identification. The values of the constants are shown in Table I, and it is interesting to note that the ratio of G/H is the value suggested by Wallmersperger *et al.*[6] Equations (1)–(4) are described only for the pure Nafion™ and Pt diffusion domain (see Fig. 1). There is neither ion diffusion nor migration in the thin Pt coating domain.

To relate the force in Eq. (4) to the physical bending of an IPMC sheet, we introduce a set of continuum mechanics equations that are effective in all domains (Fig. 1). These

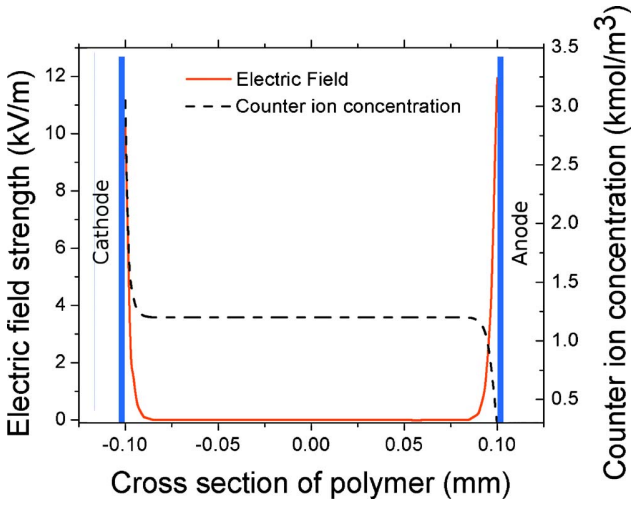

FIG. 2. (Color online) The concentration of counterions and the electric field strength inside the polymer according to simulations for a potential of 2 V.

TABLE II. Material parameters used in continuum mechanics equations.

Parameter	Value	Unit	Domain where applied
E_x	200	MPa	Nafion™
ν_N	0.49	···	Nafion™
E_{Pt}	168	GPa	Pt
ν_{Pt}	0.38	···	Pt
E_{diff}	84	Gpa	Pt diffusion layer (estimated)
ν_{diff}	0.42	···	Pt diffusion layer (estimated)

equations are described in the COMSOL MULTIPHYSICS structural mechanics software package. Normal and shear strains are defined as

$$\varepsilon_i = \frac{\partial u_i}{\partial x_i}, \quad \varepsilon_{ij} = \frac{1}{2}\left(\frac{\partial u_i}{\partial x_j} + \frac{\partial u_j}{\partial x_i}\right), \tag{5}$$

where u is the displacement vector, x denotes a coordinate, and indices i and j range from 1 to 3 and denote components in the x, y, or z direction correspondingly. The stress-strain relationship is

$$\sigma = D\varepsilon, \tag{6}$$

where D is a 6×6 elasticity matrix, consisting of the components of Young's modulus and Poisson's ratio. The system is in equilibrium if the relation

$$-\nabla\cdot\sigma = \mathbf{F} \tag{7}$$

is satisfied. This is Navier's equation for displacement. The values of Young's modulus and Poisson's ratios, which are used in the simulations, are shown in Table II. The values for the platinum diffusion region are not measured but, instead, estimated as an average of values of the pure Nafion™ and Pt region.

As our simulations are dynamic rather than static, we have to introduce an equation to describe the motion of an IPMC sheet. To do that, we use Newton's second law as follows:

$$\rho\frac{\partial^2\mathbf{u}}{\partial t^2} - \nabla\cdot c\,\nabla\mathbf{u} = \mathbf{F}, \tag{8}$$

where the second term is Navier's static equation and c is Navier's constant for a static Navier equation. The first term in Eq. (8) introduces the dynamic part of the problem. Several authors have reached the conclusion that IPMC materials exhibit viscoelastic behavior,[12,13] which is especially noticeable during high frequency movements.[14] However, we include the viscoelastic term in our equations by means of the Rayleigh damping[15] model, which is described for a one-degree-of-freedom system as follows:

$$m\frac{d^2u}{dt^2} + \xi\frac{du}{dt} + ku = f(t), \tag{9}$$

where the damping parameter ξ is expressed as $\xi=\alpha m-\beta k$. The parameter m is mass, k is stiffness, and α and β are the correspond damping coefficients. The equation for the multiple degrees of freedom is

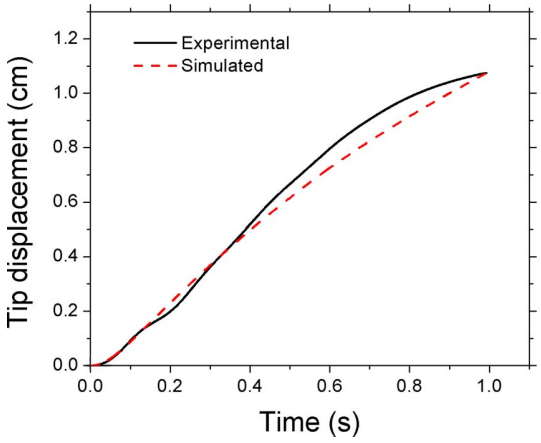

FIG. 3. (Color online) Experimental and simulation results of tip displacement. The simulation is done for a potential of 2 V. Although there is a slight difference in graphs in the large displacement region, the model gives a precise estimation for smaller displacement.

$$\rho\frac{\partial^2\mathbf{u}}{\partial t^2} - \nabla\cdot\left[c\,\nabla\mathbf{u} + c\beta\,\nabla\frac{\partial\mathbf{u}}{\partial t}\right] + \alpha\rho\frac{\partial\mathbf{u}}{\partial t} = \mathbf{F}. \tag{10}$$

By coupling Eq. (10) with the previous equations, a good basic model for the IPMC actuation has been obtained. The damping equation is very necessary to accurately describe the movement of an IPMC strip. Although the values of the parameters α and β are empirical (see Table I), they have an important role in improving the dynamical behavior of the model for nonconstant applied voltages.

All of the values used in the simulations are specified in Tables I and II. Figure 3 shows a comparison between the simulation and an actual experiment.[16] Additional comparative figures are introduced in the next section.

MODELING SELF-OSCILLATIONS

We have conducted a series of tests with IPMCs with a constant electric field in formaldehyde (HCHO) solution. Measurements show that the current oscillations begin from an applied potential of about 0.75 l. More information about the experiments and their conclusions are described in a previous paper.[9] The studies demonstrate that there are sequential electrochemical reactions taking place on the platinum cathode. The initial burst of the current is caused by the reaction

$$\mathrm{CO_{ads}} + \mathrm{OH_{ads}} \rightarrow \mathrm{CO_2} + \mathrm{H^+} + e^- + 2*, \tag{11}$$

where the subscript ads denotes species adsorbed on the platinum and · denotes an active platinum site. The result of reaction (11) is the clearing up of two platinum sites, which causes co to adsorb again. Chronopotentiometry scans show that before reaction (11), the following reactions occur:

$$\mathrm{HCHO} + * \rightarrow \mathrm{Pt\text{-}CHO_{ads}} + \mathrm{H^+} + e^-, \tag{12}$$

$$\mathrm{Pt\text{-}CHO} \rightarrow \mathrm{Pt\text{-}CO_{ads}} + \mathrm{H^+} + e^-, \tag{13}$$

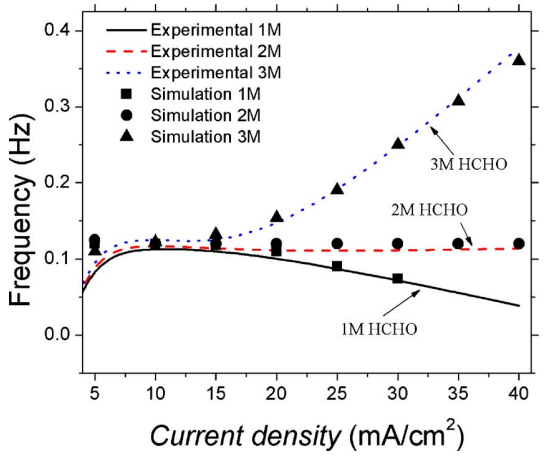

FIG. 4. (Color online) Experimental and simulated frequency dependence on the concentration of HCHO and the applied current density. Simulations for 1*M* HCHO concentration do not go past 30 mA/cm^2, because the given equation system did not give reasonable results beyond that current density.

$$H_2O + * \leftrightarrow \text{Pt-OH}_{ads} + H^+ + e^-, \tag{14}$$

HCHO is dissociated on the electrode surface at lower anodic potentials. Higher anodic potentials cause dehydrogenation of the water, resulting in water oxidation with an intermediate Pt-OH formation. We believe that these reactions lead to oscillating potentials, which, in turn, lead to the self-oscillating motion of the IPMC sheet.

A series of chronopotentiometry scans was conducted to characterize the oscillations for different HCHO concentrations and their current densities. As was discussed in our previous paper,[9] the oscillations start at approximately 7 mA/cm^2. The experiments were conducted up to the current density values of 40 mA/cm^2. Tests with HCHO concentrations of 1*M*, 2*M*, and 3*M* show that oscillation frequencies remain constant up to the current density of 14 mA/cm^2. When current is increased further in 1*M* HCHO, the frequency decreases; in 2*M* HCHO, the frequency remains constant. In the 3*M* HCHO solution, the frequency starts to increase, as shown in Fig. 4. Our goal is to develop a model to decribe the frequency behavior that is dependent on the HCHO concentration and the current density. The basic model and concepts are introduced by Kim[17] and Strasser *et al.*[18] To describe the oscillations, four dynamic parameters and, therefore, four differential equations must be observed: the concentrations of adsorbed OH and CO, the change of the double layer potential due to electrochemical reactions, and the change of the concentration of HCHO near the surface of platinum. First, two variables are expressed for a certain current density and HCHO concentration as follows:[17]

$$\dot{\theta}_{CO} = k_2 M - k_4 \theta_{CO} \theta_{OH}, \tag{15}$$

$$\dot{\theta}_{OH} = k_3 \theta_{CO} M - k_{-3} \theta_{OH} - k_4 \theta_{CO} \theta_{OH}, \tag{16}$$

where θ_{CO} and θ_{OH} are the normalized adsorption coverages of CO and OH. Variables k and M are described by the following equations:

$$k_i(\phi) = \exp[s_i(\phi - \phi_i)], \tag{17}$$

$$M = (1 - \theta_{CO} - \theta_{OH}), \tag{18}$$

where s_z are modeling coefficients and ϕ_z are potentials of the reactions.[17] The highly dynamic model introduces the double layer with thickness δ near the platinum electrode. At the far end of the layer, the concentration of the formic acid is considered constant and, due to the adsorption of HCHO on Pt, the concentration of the solution changes near the electrode. There are two components responsible for the decrease in the concentration. The first one is the direct oxidation of the formic acid to CO_2 and $2H^{\phi}$; the second one is the adsorption of CO on the platinum surface due to electrochemical reactions.[18] The mechanism that restores the HCHO concentration near the surface is diffusion. The amount of the formic acid decreases significantly when the adsorption rate is high and increases due to the diffusion during the low adsorption period. The equation describing the diffusion process is

$$\frac{\partial c_{FA}}{\partial t} = \nabla \cdot (D_{FA} \nabla c_{FA}), \tag{19}$$

with a constant concentration at the far end of the double layer and flux

$$f = k_2 M (1 + k c_r) S_{tot} \tag{20}$$

as a boundary condition on the electrode. Here, S_{tot} denotes the total number of the platinum sites per surface area. ζ_r is the normalized concentration near the boundary layer and is equal to $\zeta_r = c_{FA}/C_O$, where C_O is the initial concentration. The variable k is a simulation constant. The second term in Eq. (20) represents a simplified version of the direct oxidation path.[18] By considering these equations and the interesting nature of the frequency characteristic for different concentrations of HCHO (Fig. 4), we can now describe the empirical gray box[19] equation for the last dynamic variable—the double layer potential-as follows:

$$\dot{\phi} = \frac{1}{c_{dl}}[j_{th} - j_d + ABj^2(-j - j_{th})c_r - S_{tot}F(k_1 M + k_4 \theta_{CO} \theta_{OH})], \tag{21}$$

where j is the applied current density, j_{th} is the threshold current density with an approximate value of 10 mA/cm^2, and j_d is the direct current density and is proportional to the second term in Eq. (20). The variable B is explicitly written as $B = c_o - c_{natural}$, where $c_{natural}$ corresponds to a concentration of 2*M*. This is denoted as a "natural" concentration, as shown in Fig. 4. The oscillation frequency for the case $c_o = c_{natural} = 2M$ does not depend on the applied current density. The numeric data can be found in Table III. The third term in Eq. (21) is empirical and reflects the intriguing behavior of the oscillation frequencies for the different formic acid concentrations. Other terms are similar to the ones described by Strasser *et al.*:[18] however, some values are adjusted to get realistic simulation results. The comparison of the measured voltage oscillation with the simulation data can be seen in Fig. 5. The simulation does not require any change in the boundary or initial conditions of the basic model, which is described in the previous section. Equations (15)–(17) and

TABLE III. Variables and values used in the simulation of electrochemical oscillations.

Parameter	Value	Unit
S_{tot}	0.5×10^{-5}	mol/cm^2
C_{dl}	1	mF/cm^2
A	1.2	$cm^7/(mA^2\,mol)$
k	100	⋯
ε[a]	2×10^{-2}	cm
D_{Fa}[a]	2.5×10^{-5}	cm^2/s
$\phi_{1,2,3-3,4}$[b]	[0.2, 0.3, 0.01, 0.512, 0.77]	V
$S_{1,2,3-3,4}$[b]	[10, −11, 9, −9, 20]	V^{-1}

[a]Reference 18.
[b]Reference 17.

(21) are simulated using the weak form of the differential equation on the anode boundary.

By using the obtained voltage output in the base FEM, described in the previous section, one can simulate the oscillating deflection of an IPMC muscle. Two sample results for the different HCHO concentrations and current densities are shown in Figs. 6 and 7. As can be seen, the amplitude, frequency, and, for the most part, the shape of the deflection show a reasonable agreement between the modeling and the experimental data. There is disharmony at the areas of maximum deflection. The experiments show distinctly sharp deflections in comparison to the smoother simulation results.

SUMMARY AND CONCLUSIONS

We have developed a FEM to simulate the actuation of an IPMC. The model is largely based on physical quantities and well known or measurable variables. The migration and diffusion of the counterions inside the Nafion™ polymer are described by using the electric field change caused by the charge imbalance. This, in turn, is coupled with continuum mechanics and dynamics equations, forming a complete system of equations to describe the bending of an IPMC sheet.

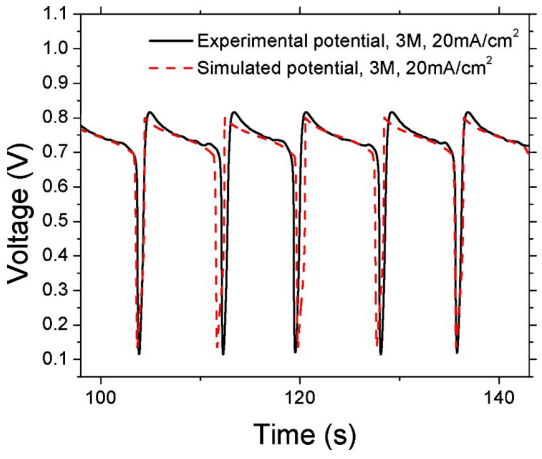

FIG. 5. (Color online) Potential oscillations. Measured data (Ref. 17) and simulated data for the 3*M* HCHO solution. The potential oscillations were measured between the cathode and anode of the IPMC strip during the experiment. The applied current was maintained at a constant value of 20 mA/cm^2.

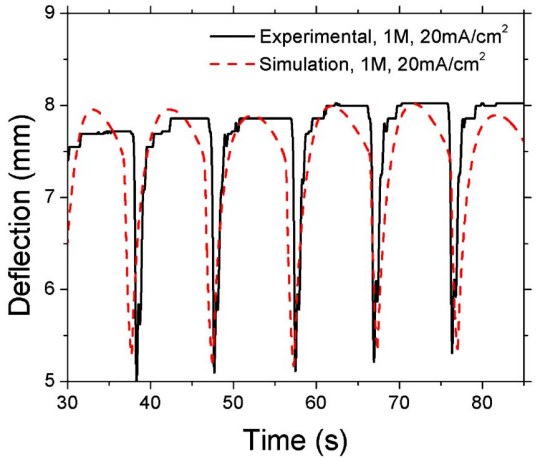

FIG. 6. (Color online) Oscillating tip displacement. Experimental (Ref. 17) data and simulation data for 1*M* HCHO solution and an applied current density of 20 mA/cm^2.

The comparison of the experimental and simulated tip displacements in time shows reasonable agreement, especially in smaller deflections. Future work will include more precise simulations for large displacements, possibly including equations that describe the voltage distribution on the surface of the electrodes that are dependent on the curvature of the IPMC. Observing the surrounding environment of the IPMC could be a factor in the next series of experiments.

The second part of the work describes the extended model for self-oscillating IPMCs. The oscillations occur when a platinum-coated IPMC is immersed into HCHO containing solutions and subjected to a constant potential or current. The extended model takes into account the changes in the HCHO concentration as it nears the electrode and the poisoning level of the platinum sites. This, in turn, results in the oscillating double layer potential, which is used in the base model to calculate the time-dependent tip displacement of the IPMC muscle. Most of the time, the model follows the simulation data closely. The experimental deflection demonstrated distinctly sharp movements at certain regions, but the

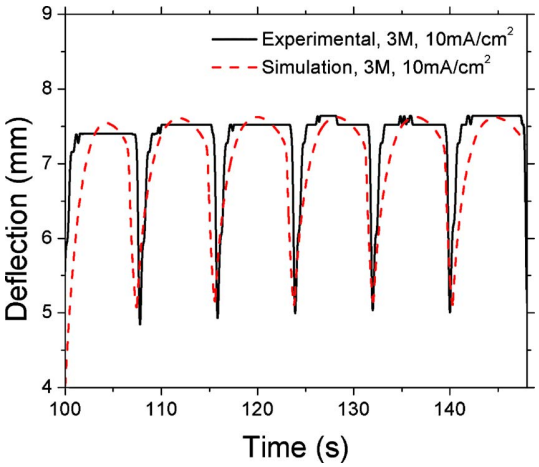

FIG. 7. (Color online) Oscillating tip displacement. Experimental (Ref. 17) data and simulation data for 3*M* HCHO solution and an applied current density of 10 mA/cm^2.

simulation gives smoother displacement profiles. Future work will include further studies on this interesting behavior in order to improve the model.

ACKNOWLEDGMENTS

We want to acknowledge the support of the US Office of Naval Research (N00014-04-0673) and Estonian Science Foundation Grant Nos. 6763 and 6765. Also we acknowledge the Estonian Archimedes Foundation for travel support of D.P. to the University of Nevada, Reno.

[1]M. Shahinpoor and K. J. Kim, Smart Mater. Struct. **10**, 819 (2001).
[2]T. Wallmersperger, B. Kroplin, and R. W. Gulch, Mech. Mater. **36**, 411 (2004).
[3]S. Nemat-Nasser and S. Zamani, J. Appl. Phys. **100**, 064310 (2006).
[4]Y. Toi and S.-S. Kang, Comput. Struct. **83**, 2573 (2005).
[5]S. Lee, H. C. Park, and K. J. Kim, Smart Mater. Struct. **14**, 1363 (2005).
[6]T. Wallmersperger, D. J. Leo, and C. S. Kothera, J. Appl. Phys. **101**, 024912 (2007).
[7]B. Miller and A. Chen, J. Electroanal. Chem. **588**, 314 (2006).
[8]K. Krischer, J. Electroanal. Chem. **501**, 1 (2001).
[9]D. Kim, K. J. Kim, Y. Tak, D. Pugal, and I.-S. Park, Appl. Phys. Lett. **90**, 184104 (2007).
[10]S. Nemat-Nasser and Y. Wu, J. Appl. Phys. **93**, 5255 (2003).
[11]S. Nemat-Nasser and J. Y. Li, J. Appl. Phys. **87**, 3321 (2000).
[12]K. M. Newbury and D. J. Leo, J. Intell. Mater. Syst. Struct. **14**, 333 (2003).
[13]K. Yagasaki and H. Tamagawa, Phys. Rev. E **70**, 052801 (2004).
[14]K. M. Newbury and D. J. Leo, J. Intell. Mater. Syst. Struct. **14**, 343 (2003).
[15]J. W. S. Rayleigh, *The Theory of Sound* (Dover, New York, 1945), Vol. 2, p. 226.
[16]A. Punning, M. Kruusmaa, and A. Aabloo, Sens. Actuators, A **133**, 200 (2007).
[17]D. Kim, Ph.D. thesis, University of Nevada, Reno, 2006.
[18]P. Strasser, M. Eiswirth, and G. Ertl, J. Chem. Phys. **107**, 991 (1997).
[19]M. Shahinpoor and K. J. Kim, Smart Mater. Struct. **13**, 1362 (2004).